

Research Article

Research on the Disintegration Characteristics of Carbonaceous Mudstone and Properties of Modified Materials

Xinxi Liu, Yu Li^{ID}, Shengnan Li, and Yanming Zhou

School of Civil Engineering, Changsha University of Science & Technology, Changsha 410114, China

Correspondence should be addressed to Yu Li; 1986740197@qq.com

Received 29 May 2019; Revised 16 September 2019; Accepted 22 October 2019; Published 9 December 2019

Academic Editor: Abdul Aziz bin Abdul Samad

Copyright © 2019 Xinxi Liu et al. This is an open access article distributed under the Creative Commons Attribution License, which permits unrestricted use, distribution, and reproduction in any medium, provided the original work is properly cited.

This work presents the results of an experimental investigation aimed to study the disintegration of carbonaceous mudstone and properties of modified materials. The mineralogical composition of carbonaceous mudstone was determined with X-ray diffraction. The microscopic characteristics of carbonaceous mudstone disintegration were determined with scanning electron microscopy. The surface modification effect of carbonaceous mudstone was researched by comparative tests on coatings' hydrophobic property, fastness, and waterproof before and after modification, and the modification mechanism of polymer-cement composite modified carbonaceous mudstone was analyzed. The results show that the mineral composition of carbonaceous mudstone mainly contains illite, quartz, and kaolinite. It is found that the disintegration of carbonaceous mudstone can be divided into external factors and internal factors. External factors are water and temperature difference, and internal factors are the swelling of the kaolinite and illite mineral particles. There are differences in the modification effects under different cement dosage. When the cement dosage is 30%, the modification effect is the best. The results may provide a reference for the prevention and control of soft rock slopes.

1. Introduction

In recent years, with the implementation of China's "The Belt and Road" strategy, roads, railways, and other infrastructure in the southwest of China, where carbonaceous mudstone is widely distributed, have developed rapidly. However, the carbonaceous mudstone cutting slope, under the coupled action of heat-water-force-chemistry and other factors, will produce crack and disintegration (Figure 1), which is easy to cause shallow instability and even induce engineering geological disasters such as expressway cutting slope collapse and landslide, seriously affecting the progress of the project, safety of staff, and economic losses [1, 2]. Therefore, domestic and foreign scholars have carried out a series of experiments and theoretical studies on soft rock and obtained fruitful research results. Ganesh et al. [3] studied the influence of the mineral composition on the disintegration resistance of soft rock. Zhang et al. [4] analyzed the influence of swelling rock with drying-wetting cycles on stability of canal slope through laboratory and centrifuge

model tests. Pan et al. [5] quantitatively characterized the disintegration process of soft rock in water by establishing the interface model of soft rock with water disintegration. It was found that the crack propagation of carbonaceous mudstone can be divided into three stages: slow development, rapid development, and stable development by laboratory tests [6]. Wong and Wang [7] constructed a three-dimensional mathematical model to simulate the expansion of argillaceous rock by considering the three elements of mineral particle expansion, fabric, and stress-induced anisotropy. Some researchers discussed the influence of strain change and number of dry and wet cycles on expansive force based on the expansion test of argillaceous rock [8–10]. From the perspective of energy, the energy transfer and energy dissipation model of the process of soft rockfall was established through quantitative characterization of the process [11]. More recently, scanning electron microscopy and X-ray diffraction have been used to analyze the characteristics of soft rock disintegration. For example, Zeng et al. [12] obtained that the mesodamage evolution of



FIGURE 1: Failure mode of carbonaceous mudstone. (a) Cracking type. (b) Carbonaceous mudstone after disintegration.

carbonaceous mudstone under the action of confining pressure and deviatoric stress was a nonlinear cumulative growth process based on CT-triaxial test. Chai et al. [13] analyzed the relationship between the disintegration resistance of mudstone and mineral composition. Vgerara et al. [14] analyzed the effect of water content on the mechanical properties of argillaceous expansive rocks. A mathematical model was established based on the disintegration test, which is used to describe the variation rule of the disintegration index with the increase of the number of dry and wet cycles [15]. Undoubtedly, the above research provides an important reference for the disintegration and disintegration mechanism of soft rock.

At present, domestic and foreign scholars have studied how to improve the stability of tunnel, chamber, slope, and other geotechnical engineering, and the research results have achieved good results [16–23]. However, there are few research studies on improving the stability of soft rock and soft rock engineering. Therefore, this paper takes the carbonaceous mudstone slope of the Liuzhai-Hechi expressway in Guangxi city, China, as the research object. A new kind of polymer-cement composite was synthesized by radical solution and sol-gel method. Verified by a case study, the results may provide a reference for the prevention and control of soft rock slopes.

2. Disintegration Experiment of Carbonaceous Mudstone

2.1. Chemical Composition of Specimens. The carbonaceous mudstone used in the test was taken from the K24 + 400 station of the Liuzhai-Hechi expressway in Guangxi city, China. The carbonaceous mudstone was analyzed by X-ray diffraction. The X-ray diffraction spectrum is shown in Figure 2. The mineral composition is shown in Figure 3. It can be seen from Figure 3 that the mineral composition of carbonaceous mudstone mainly contains quartz, illite, and kaolinite, and the mass percentage of other mineral components is less than 7%. As kaolinite and illite are highly hydrophilic clay minerals, the carbonaceous mudstone is easily softened and disintegrated in water.

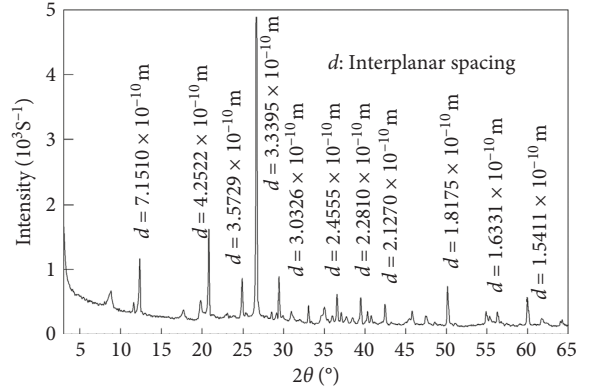


FIGURE 2: X-ray diffraction spectrum of carbonaceous mudstone.

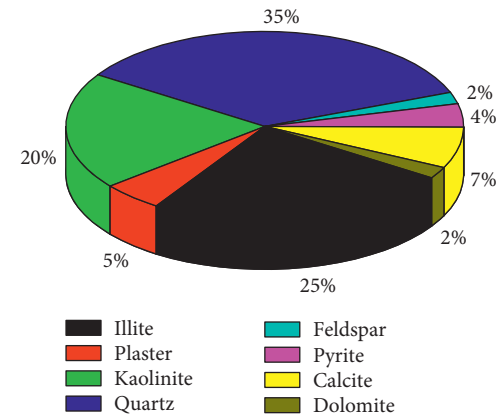


FIGURE 3: Mineral composition of carbonaceous mudstone.

2.2. Experiment Method. In order to comprehensively study the disintegration characteristics of the carbonaceous mudstone, an experimental scheme was designed from three treatment modes, i.e., water action, heat action, and water-heat interaction. According to the test specifications [24], the carbonaceous mudstone is composed of 10 round samples with a mass of 40~60 g, as shown in Figure 4. After each cycle, sieves of 40 mm, 20 mm, 10 mm, 5 mm, 2 mm, 0.5 mm, 0.25 mm, 0.075 mm, and other specifications were used to



FIGURE 4: Photographs of the test samples.

screen and record the particle grade. Various treatment methods are as follows:

- (1) Under the action of water: the selected sample was weighed and placed in an open container, and the sample was completely immersed in water for 24 hours by water injection. The disintegration was obtained by using a standard sieve and placed outside to dry until the quality of the disintegration remained unchanged. Each cycle is from soaking to drying.
- (2) Under the action of heat: the selected sample was weighed and placed in an oven at 105°C for 24 hours. The disintegration was then taken out and cooled to room temperature.
- (3) Under the action of water-heat: the selected sample was weighed and placed in an open container, and the sample was completely immersed in water for 24 hours by water injection. The disintegration was obtained by using a standard sieve and placed in an oven at 105°C until the quality of the disintegration remained unchanged.

Under the above three conditions, the weight of each particle size is a cycle, and 5 cycles are carried out under each condition.

2.3. Distribution Characteristics of Disintegration Particles. When the disintegration of the carbonaceous mudstone was completed, the disintegrating particles were analyzed. The percentage of disintegrating particles of the carbonaceous mudstone under different conditions was obtained as shown in Figure 5.

When the disintegration was basically stable, it can be seen from Figure 5 that the particles were mainly distributed in the particle size of 0.5~5 mm under the action of water and water-heat. The disintegrating particles with a particle size less than 2 mm account for 37.82% under the action of water and 54.41% under the action of water-heat. During the cycle of heat, the disintegration of the carbonaceous mudstone is very small and almost not disintegrated, which is consistent with the results of Yamaguchi et al. [25]. The results show that the effect of water-heat action on the disintegration of the carbonaceous mudstone is greater than

that of water or heat, and the temperature difference can accelerate the disintegration rate of the carbonaceous mudstone based on the condition of water.

2.4. Microscopic Characteristics of Carbonaceous Mudstone Disintegration. Studying the characteristics of microstructure changes during the softening and disintegration of carbonaceous mudstones has important guiding significance for the formulation of engineering stability technical countermeasures. At present, scanning electron microscopy (SEM) is one of the main instruments for material microscopy research, which is widely used in geotechnical engineering. In this paper, SEM was used to observe the carbonaceous mudstone under different soaking conditions, as shown in Figure 6.

According to scanning electron microscopy, the natural carbonaceous mudstone sample has a good integrity and its rock particles are tightly cemented (see Figure 6(a)). The main reason is that the coarse grain skeleton, which is composed of quartz, mica, feldspar, and other mineral particles, was filled with clay particles such as illite and kaolinite with smaller grain size, which acts as cementation to make the structure compact. When the sample was immersed for the first day, the microstructure of the sample did not change and the structure was stable (Figure 6(b)). When the sample was immersed for the second day, a large number of clay particles were exposed and shed, which caused the destruction of rock microstructure (Figure 6(c)). When the sample was immersed for the seventh day, the sample was transformed from an initial compact structure to a loose flocculated structure (Figure 6(d)). Compared with the soaking condition, the clay particle was shed more quickly and the microstructure was destroyed more seriously under the condition of drying-wetting circulation (Figures 6(e) and 6(f)). The results show that the disintegration of the carbonaceous mudstone in water is closely related to the microstructure change of the carbonaceous mudstone, and the disintegration of the carbonaceous mudstone can be accelerated under the action of drying-wetting circulation.

3. Analysis of Properties and Mechanism of Modified Materials

3.1. Modified Material Preparation. The modified material used in the test is a polymer-cement composite curing agent, which is composed of epoxy resin emulsion, cement, and polyether-modified silicone. The composition of the modified material is shown in Table 1. The preparation process of the modified material is as follows:

- (1) The weighed epoxy resin emulsion and water were stirred for 30 s at a low speed, and the stirring method was carried out by the prewetting method
- (2) The weighed cement and polyether-modified silicone defoaming agent were added in the low-speed stirring process, and the stirring time was 120 s
- (3) Stirring was continued by hand and then shaken evenly manually

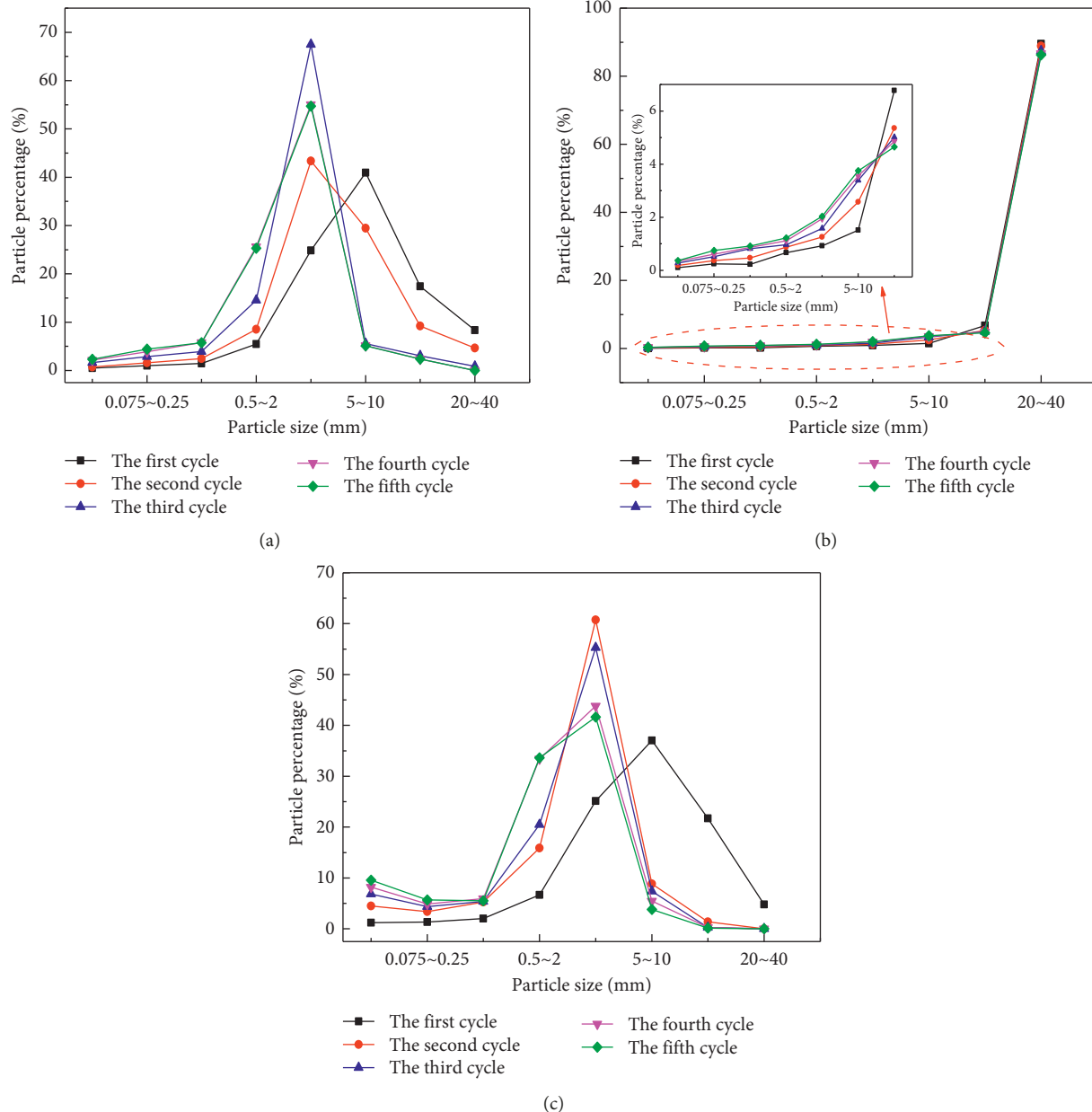


FIGURE 5: Percentage of disintegrating particles of the carbonaceous mudstone under different conditions. (a) Under the action of water. (b) Under the action of heat. (c) Under the action of water-heat.

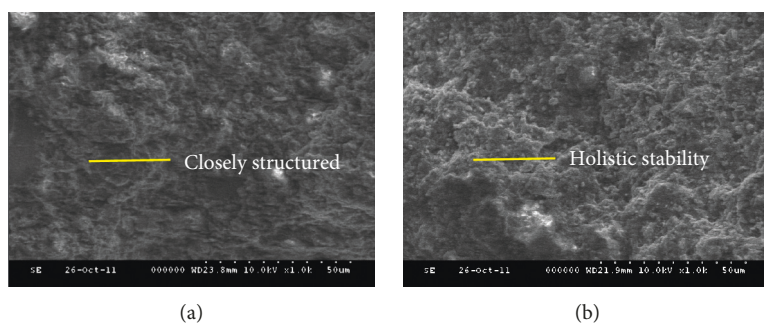


FIGURE 6: Continued.

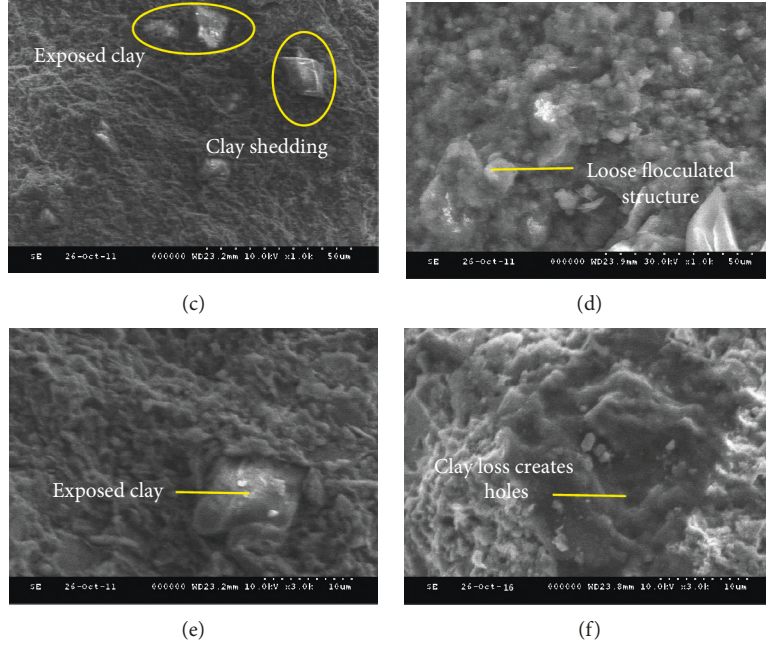


FIGURE 6: Microscopic view of carbonaceous mudstone under different immersion times. (a) Natural state ($\times 1000$ times). (b) The first day ($\times 1000$ times). (c) The second day ($\times 1000$ times). (d) The seventh day ($\times 1000$ times). (e) The second day ($\times 3000$ times). (f) The second day of the drying-wetting cycle ($\times 3000$ times).

TABLE 1: Composition of the modified material.

Number	Epoxy emulsion quantity (g)	Water quantity (g)	Cement quantity (g)	Silicone defoamer (%)	Cement dosage (cement: epoxy emulsion) (%)
A0	100	25	0	1	0
A1	100	25	10	1	10
A2	100	25	20	1	20
A3	100	25	30	1	30
A4	100	25	40	1	40
A5	100	25	50	1	50

3.2. Hydrophobic Performance. The contact angle was effectively used to characterize the hydrophobic properties of the material surface. The contact angle was determined by the static water contact method according to the Chinese Standard GB/T 30693-2014 [26]. Under the dry conditions at room temperature, the contact angle of unmodified and modified samples was measured by using the contact angle measuring instrument. The shape of the water droplet on the surface of unmodified and modified samples is shown in Figure 7. The measured results of the surface contact angle of unmodified and modified samples are shown in Table 2.

It can be seen from Figure 7 that the water droplet on the surface of the unmodified sample was convex lenticular, while that of the modified sample was hemispherical. As can be seen from Table 2, the contact angle of the modified sample increased obviously and the variation was $42.3^\circ \sim 50.1^\circ$. When the cement dosage was 30%, the change of the contact angle was the largest and the hydrophobic performance was the best. It is shown that the polymer-cement composite can change the surface structure and

properties of the rock sample effectively and make the surface change from hydrophilic to hydrophobic.

3.3. Film Performance. The firmness between the membrane layer and the rock surface was generally measured by the method of scratch according to the Chinese Standard GB1720-1979 [27]. First, the scratch tool was used to scratch 100 squares with a side length of 1 mm on the rock surface and glued the tape. After quickly removing the cementation tape, the film shedding between scratches was observed as shown in Figure 8.

The percentage of film shedding was used to measure the firmness between the membrane layer and the rock surface. To study the influence of cement dosage on the bond strength, the relationship between the cement dosage and the percentage of film shedding was plotted, as shown in Figure 9.

Figure 9 shows that the percentage of film shedding on the modified rock surface was decreased. The bond strength between the membrane layer and the rock surface was

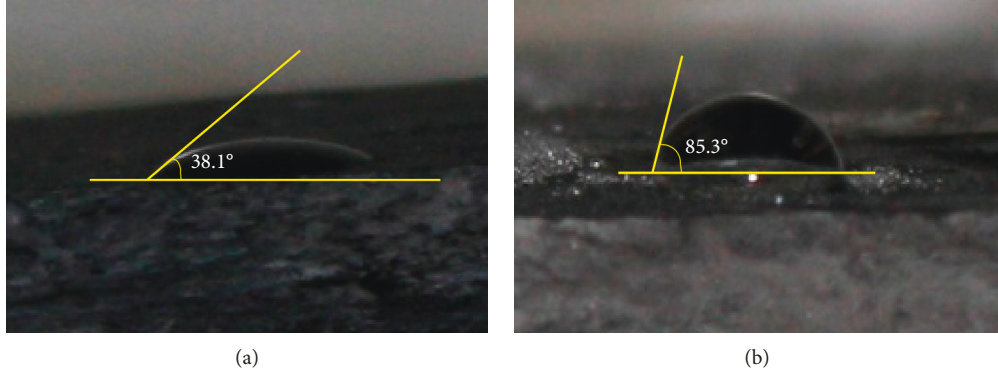


FIGURE 7: Photos of the water droplet on the soft rock surface. (a) Unmodified sample. (b) Modified sample.

TABLE 2: Measured results of the contact angle on the sample's surface.

Number	Unmodified	Contact angle (°)		Amount of change
		Modified	Unmodified	
A1	38.1	85.3	38.1	47.2
A2	35.0	83.1	35.0	48.1
A3	32.8	82.9	32.8	50.1
A4	34.4	80.8	34.4	46.4
A5	35.6	77.9	35.6	42.3

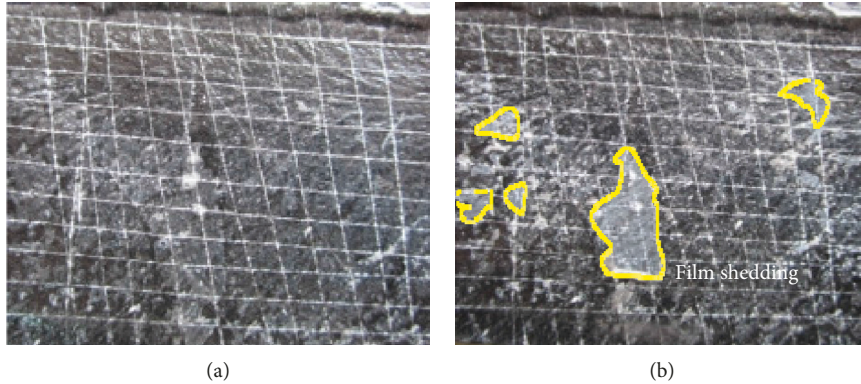


FIGURE 8: Photos showing the scratches on the membrane layer. (a) Rules of the graphics after scratch. (b) Shedding situation of the membrane layer.

improved. It is found that the firmness of the film layer does not increase with the increase of the cement dosage, but shows a trend of increasing gradually and then decreasing, indicating that the film surface stability of the rock sample was not better with the increase of cement content. By fitting the test data, it is found that the relationship between the cement dosage and the percentage of film shedding is in accordance with the GaussAmp function distribution. The fitting expression is as shown in equation (1) and the correlation coefficient $R = 0.986$:

$$y = 27.71 - 25.42e^{-(x-31.19/20.23\sqrt{2})^2}. \quad (1)$$

Comparing the fitting curve and the experimental data, it can be seen that when the cement dosage is about 30%, the percentage of film shedding was the smallest, the bond

strength between the rock surface and the film layer was the largest, and the film layer was the strongest.

3.4. Waterproof Performance. The waterproof performance of modified materials was determined by a water absorption test. The water absorption rate was used to characterize the surface waterproof performance of rock samples, and the water absorption rate is the ratio of the water absorption weight to the dry weight of the rock sample. The variation curve of the water absorption rate of the rock sample with the immersion time under different cement contents is shown in Figure 10.

Figure 10 shows that the unmodified carbonaceous mudstone is immersed in water, the water molecules rapidly infiltrated into the interior of the rock sample, and the water

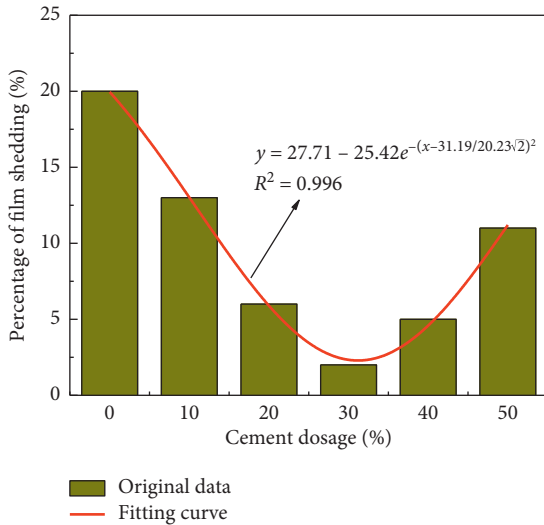


FIGURE 9: The relationship between the cement dosage and the percentage of film shedding.

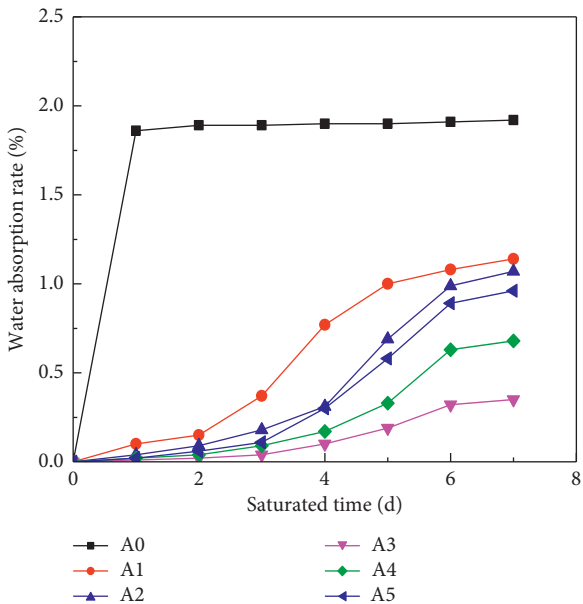


FIGURE 10: Curve of water absorption of the sample with immersion time.

absorption rate increases rapidly, and a large number of bubbles were generated on the surface of the rock sample and then the water absorption rate increases slowly. After 7 days of water immersion, the water absorption rate is 1.92% and its failure form was cracking and disintegration. Since the modified material can form a reticular membrane on the surface of the rock sample, the water molecules are prevented from infiltrating into the rock sample effectively. There are differences in waterproof performance under different cement dosage. When it is 30%, the waterproof performance is the strongest and the water absorption rate of the rock sample is 0.35%, which is only 18.23% before the

modification. There is no crack on the surface of the rock sample.

3.5. Analysis of Modification Mechanism. X-ray diffraction results show that the clay mineral composition of the carbonaceous mudstone mainly contains kaolinite and illite, accounting for 45%. As the surface of kaolinite clay has free silicon, aluminum atoms, and ions, an electrostatic gravitational field is formed, so that water molecules are easily adsorbed on the clay surface, resulting in clay mineral external expansion. The crystal structure of illite is a three-layer cell. After immersion in water, the anti-ions between the crystal cells will escape and water molecules will be squeezed in. As a result, the spacing between crystal cells will expand, resulting in the expansion of clay minerals. In addition, due to the uneven distribution of expansive clay minerals in the sample, uneven expansion occurs and a large number of pores are generated, as shown in Figure 11(a).

The microstructure of the soft rock modified by the polymer-cement composite after immersion is shown in Figure 11(b). The mineral particles on the surface of the rock sample are closely bonded. This is because the polymer emulsion penetrates into the pores of the cement hydration product to form a film layer, which is intertwined with the hydration product, and the polymer particles are fused together to form a cautious water film of the network structure. The bond strength and waterproof performance between the modified material and the soft rock surface are improved, thereby improving the permeability and softening disintegration of the carbonaceous mudstone, which has important practical significance for the development of the soft rock slope engineering.

4. Typical Case Analysis

A field application of the polymer-cement composite curing agent in the K24 + 400 station of the Liuzhai-Hechi expressway cutting slope in Guangxi city, China, was studied with the modification effect. From the experimental results, the polymer-cement composite with a cement dosage of 30% is adopted to cure the soft rock slope. The process of construction technology is shown in Figure 12.

There are some findings at the construction site: by curing the carbonaceous mudstone slope and spraying grass seeds in the outside soil, the weathering and disintegration of carbonaceous mudstone can be effectively prevented. The grass seeds have basically sprouted at the construction site by observing, and the rate of germination reached 90%. After several months of maintenance, the vegetation on the slope grew well and the slope was in the steady state, as shown in Figure 13(a). When the carbonaceous mudstone slope is not solidified, the vegetation on the slope is poorly grown and the carbonaceous mudstone on the slope is cracked, as shown in Figure 13(b). The engineering example shows that polymer-cement composites are feasible to solve the stability problem of the carbonaceous mudstone slope.

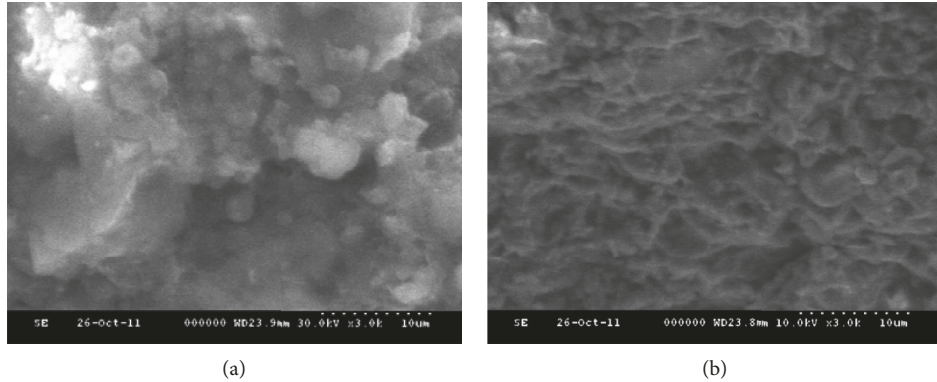


FIGURE 11: Micrograph of the carbonaceous mudstone before and after modification. (a) Before curing ($\times 3000$ times). (b) Cement dosage is 30%.



FIGURE 12: Construction technology process.



FIGURE 13: The effect of slope protection under different conditions. (a) Cured slope. (b) Slope without curing.

5. Conclusions

The experimental investigation of disintegration and modification of carbonaceous mudstone is presented in this paper. The disintegration characteristics and properties of modified materials are studied. The following conclusions can be drawn based on this study:

- (1) It can be seen from the disintegration experiment of the carbonaceous mudstone that water and temperature

difference are external factors affecting the disintegration of the carbonaceous mudstone, while kaolinite and illite clay minerals are the internal factors leading to the disintegration of the carbonaceous mudstone.

- (2) The carbonaceous mudstone before modification was easy to soften and disintegrate in water, and its mesoscopic characteristics change from dense structure to loose and irregular floc structure. After the modification of the polymer-cement composite,

- the hydrophobic, binding, and waterproof properties of the carbonaceous mudstone were improved, and the microscopic characteristics show that the mineral particles are closely bound together.
- (3) There are differences in the modification effects under different cement dosage. When the cement dosage is 30%, the modification effect is the best. The engineering example shows that polymer-cement composites are feasible to solve the stability problem of the carbonaceous mudstone slope.
- ## Data Availability
- The data used to support the findings of this study are included within the article.
- ## Conflicts of Interest
- The authors declare that they have no conflicts of interest regarding the publication of this paper.
- ## Acknowledgments
- This work was supported by the National Natural Science Foundation of China (51674041) and the Postgraduate Research and Innovation Project of Hunan Province (CX20190657).
- ## References
- [1] M. C. He, H. H. Jing, and X. M. Sun, *Engineering Mechanics of Soft Rock*, Science Press, Beijing, China, 2002.
 - [2] J. H. Yang, F. Q. Wu, D. Wang et al., "Research on collapse of high cutting slope with horizontal soft-hard alternant strata in Three Gorges reservoir area," *Rock and Soil Mechanics*, vol. 31, no. 1, pp. 151–157, 2010.
 - [3] D. Ganesh, Y. Tesuro, K. Masaji, and K. Katsuhiko, "Slake durability and mineral-logical properties of some pyroclastic and sedimentary rocks," *Engineering Geology*, vol. 6, no. 5, pp. 31–45, 2002.
 - [4] C. Zhang, Z. Y. Cai, Y. H. Huang, and H. Chen, "Laboratory and centrifuge model tests on influence of swelling rock with drying-wetting cycles on stability of canal slope," *Advances in Civil Engineering*, vol. 2018, Article ID 4785960, 10 pages, 2018.
 - [5] Y. Pan, Z. Liu, and C. Y. Zhou, "Experimental study of disintegration characteristics of red-bed soft rock within water and its interface model," *Rock and Soil Mechanics*, vol. 38, no. 11, pp. 3231–3239, 2017.
 - [6] L. Zeng, J. Liu, Q. F. Gao, and H. Bian, "Evolution characteristics of the cracks in the completely disintegrated carbonaceous mudstone subjected to cyclic wetting and drying," *Advances in Civil Engineering*, vol. 2019, Article ID 1279695, 10 pages, 2019.
 - [7] R. C. K. Wong and E. Z. Wang, "Three-dimensional anisotropic swelling model for clay shale -a fabric approach," *International Journal of Rock Mechanics and Mining Sciences*, vol. 34, no. 2, pp. 187–198, 1997.
 - [8] O. J. Pejon and L. V. Zuquette, "Effects of strain on the swelling pressure of mudrocks," *International Journal of Rock Mechanics and Mining Sciences*, vol. 43, no. 5, pp. 817–825, 2006.
 - [9] O. J. Pejon and L. V. Zuquette, "Analysis of cyclic swelling of mudrocks," *Engineering Geology*, vol. 67, no. 1-2, pp. 97–108, 2002.
 - [10] R. Doostmohammadi, M. Moosavi, and B. N. Araabi, "A model for determining the cyclic swell-shrink behavior of argillaceous rock," *Applied Clay Science*, vol. 42, no. 1-2, pp. 81–89, 2008.
 - [11] V. Miklúšová and L. Ivaničová, "Energetic approach to the evaluation of rock disintegration process," *Acta Montanistica Slovaca*, vol. 13, no. 1, pp. 17–24, 2008.
 - [12] L. Zeng, Z. N. Shi, H. Y. Fu et al., "Road performance of preliminary disintegration of carbon mudstone and mechanical characteristics based on CT-Triaxial test," *Journal of Central South University (Science and Technology)*, vol. 47, no. 6, pp. 2030–2036, 2016.
 - [13] Z. Y. Chai, Y. T. Zhang, and X. Y. Zhang, "Experimental investigations on correlation with slake durability and mineral composition of mudstone," *Journal of China Coal Society*, vol. 40, no. 5, pp. 1188–1193, 2015.
 - [14] M. R. Vgerara and T. Triantafyllidis, "Influence of water content on the mechanical properties of an argillaceous swelling rock," *Rock Mechanics and Rock Engineering*, vol. 49, no. 7, pp. 2555–2568, 2016.
 - [15] Z. H. Zhang, W. Liu, Q. Cui, L. Han, and H. Yao, "Disintegration characteristics of moderately weathered mudstone in drawdown area of Three Gorges Reservoir, China," *Arabian Journal of Geosciences*, vol. 2018, p. 10, 2018.
 - [16] K. Z. Zhang, J. M. Xia, and J. Q. Jiang, "Structure and application of strong shell-body support in soft rock roadway," *Chinese Journal of Rock Mechanics and Engineering*, vol. 23, no. 4, pp. 668–672, 2004.
 - [17] Q. H. Wu, L. Chen, B. T. Shen, B. Dlamini, S. Li, and Y. Zhu, "Experimental investigation on rockbolt performance under the tension load," *Rock Mechanics and Rock Engineering*, vol. 52, no. 11, pp. 4605–4618, 2019.
 - [18] Q. H. Wu, X. B. Li, L. Weng et al., "Experimental investigation of the dynamic response of prestressed rockbolt by using an SHPB-based rockbolt test system," *Tunnelling and Underground Space Technology*, vol. 93, p. 103088, 2019.
 - [19] X. Z. Hua and G. X. Xie, "Research on grouting material for bolt and grouting reinforcement of soft rock tunnel and its application," *Rock and Soil Mechanics*, vol. 25, no. 10, pp. 1642–1646, 2004.
 - [20] L. Chen, Z. L. Zhou, C. W. Zang et al., "Failure pattern of large-scale goaf collapse and a controlled roof caving method used in gypsum mine," *Geomechanics and Engineering*, vol. 18, no. 4, pp. 449–457, 2019.
 - [21] X. Wang, M.-M. Hong, Z. Huang et al., "Biomechanical properties of plant root systems and their ability to stabilize slopes in geohazard-prone regions," *Soil and Tillage Research*, vol. 189, pp. 148–157, 2019.
 - [22] J. Liu, Z. Chen, D. P. Kanungo et al., "Topsoil reinforcement of sandy slope for preventing erosion using water-based polyurethane soil stabilizer," *Engineering Geology*, vol. 252, pp. 125–135, 2019.
 - [23] G. W. Liu and S. L. Lu, "Reinforcement effect of cement grouting on engineering rock mass," *Journal of China University of Mining and Technology*, vol. 29, no. 5, pp. 454–458, 2000.
 - [24] DZ/T 0276.9-2015, *Regulation for Testing the Physical and Mechanical Properties of Rock*, Professional Standard of Geological and Mining Industry of the People's Republic of China, Beijing, China, 2015.

- [25] H. Yamaguchi, K. Yoshida, I. Kuroshima et al., *Slaking and Shear Properties of Mudstone*, Rock Mechanics and Power Plants, Rotterdam, Netherlands, 1998.
- [26] GB/T 30693-2014, *Measurement of Water-Contact Angle of Plastic Films*, National Standard of the People's Republic of China, Beijing, China, 2014.
- [27] GB1720-1979, *Determination of Film Adhesion*, National Standard of the People's Republic of China, Beijing, China, 1979.

